PERGAMON

Applied Geochemistry 17 (2002) 431–443

Applied Geochemistry

www.elsevier.com/locate/apgeochem

A geochemical model for removal of iron(II)(aq) from mine water discharges

Sean P. Burke[a,b,*], Steven A. Banwart[a,b]

[a]*Department of Geography, University of Sheffield, Sheffield, S10 2TN, UK*
[b]*Groundwater Protection and Restoration Group, Department of Civil and Structural Engineering, University of Sheffield, S1 3JD, UK*

Received 15 September 2000; accepted 1 May 2001
Editorial handling by G. Ferris

Abstract

A steady state geochemical model has been developed to assist in understanding surface-catalysed oxidation of aqueous Fe(II) by O_2(aq), which occurs rapidly at circumneutral pH. The model has been applied to assess the possible abiotic removal of Fe(II)(aq) from alkaline ferruginous mine water discharges using engineered reactors with high specific-surface area filter media. The model includes solution and surface speciation equilibrium, oxidation kinetics of dissolved and adsorbed Fe(II) species and mass transfer of O_2(g). Limited field data for such treatment of a mine water discharge were available for model development and assessment of possible parameter values. Model results indicate that an adsorption capacity between 10^{-6} and 10^{-5} mol l^{-1} is sufficient for complete removal, by oxidation, of the Fe(II)(aq) load at the discharge. This capacity corresponds approximately to that afforded by surface precipitation of Fe(III) oxide onto plastic trickling filter media typically used for biological treatment of wastewater. Extrapolated literature values for microbial oxidation of Fe(II)(aq) by neutrophilic microbial populations to the simulated reactor conditions suggested that the microbially-mediated rate may be several orders-of-magnitude slower than the surface-catalysed oxidation. Application of the model across a range of mine water discharge qualities shows that high Fe(II)(aq) loadings can be removed if the discharge is sufficiently alkaline. Additional reactor simulations indicate that reactor efficiency decreases dramatically with pH in the near acid region, coinciding with the adsorption edge for Fe^{2+} on Fe oxyhydroxide. Alkaline discharges thus buffer pH within the range where Fe(II)(aq) adsorbs onto the accreting Fe hydroxide mineral surface, and undergoes rapid catalytic oxidation. The results suggest that the proposed treatment technology may be appropriate for highly ferruginous alkaline discharges, typically associated with abandoned deep coal mines.

1. Introduction

Mine water discharges occur in many parts of the world. An estimated 11% of the global fluvial SO_4 flux arises from pyrite oxidation, and is increasing due to mining activities (Nordstrom and Southam, 1997). Recent descriptions of such discharges include those in the UK (Banks, 1996), South Africa (Clarke, 1997), France (Sadler, 1998), South Korea (Cheong et al., 1998), China (Feng et al., 2000) and the United States (Kirby et al., 1999). In the northern Appalachian Plateau of the eastern United States abandoned coal mine discharges influence in excess of 8000 km of streams and associated groundwater (Cravotta and Trahan, 1999). In 1994 the UK National Rivers Authority (now the Environment Agency) suggested that some 100 discharges were causing significant pollution problems, with 198 km of rivers, streams or brooks affected in the UK (NRA, 1994). The source of mine water discharges can be from deep or shallow mine workings, either active where dewatering is taking place or abandoned if groundwater rebound has been allowed to occur (Burke and Younger, 2000).

* Corresponding author. Fax: +44-114-2797912.
E-mail address: s.burke@sheffield.ac.uk (S.P. Burke).

0883-2927/02/$ - see front matter
PII: S0883-2927(01)00092-0

Surface runoff from mine waste is a notorious source of acidity and heavy metal contamination for streams and groundwater (Appelo and Postma, 1996; Banks et al., 1997; Licsko et al., 1999). Acidic mine waters can have a profound influence on the surrounding environment and pose a serious threat of long-term environmental degradation. Low pH and elevated concentrations of metal ions (e.g. Fe^{2+}, Mn^{2+}, Al^{3+}, Cu^{2+}, Pb^{2+}, Cd^{2+}, Zn^{2+}, etc.) and oxyanions (CrO_4^{2-}, AsO_3^{-}, etc.) often characterise these discharges (Banks et al., 1997).

On the other hand, alkaline mine waters are typical of many discharging mine waters (Banks et al., 1997), particularly those associated with mature, flooded deep mine systems (Younger, 1997). These discharges are generally not that polluting in terms of metal toxicity, but can be highly ferruginous and visibly unsightly as Fe(III) oxyhydroxide precipitates are deposited on the beds of receiving streams. Subsequent deterioration of the benthic food chain can be significant and lead to serious impacts on stream ecology. (Younger and Banwart, 1999). The particular focus of the study presented here is the treatment of alkaline discharges by removal of Fe(II)(aq) using a novel passive remediation technique.

Discharging mine waters can be treated actively or passively or by a combination of both methods. Active treatment involves the continuous addition of chemicals and/or electricity for pumping and mechanical aeration in order to reduce the contaminant loadings. For acidic discharges, lime dosing is often used to raise the pH and increase the rate of Fe(II) oxidation and the subsequent precipitation of Fe(III) oxide minerals. Aeration will also assist O_2 transfer for the oxidation of Fe^{2+} to Fe^{3+} and the subsequent removal by precipitation. However, active treatment is associated with high operating costs. Because the duration of contamination loadings are often unknown, there is an associated uncertainty in the financial liability at such sites. Consequently, active treatment using chemical addition or aeration is often not financially viable for many mine water discharges.

Passive treatment systems avoid continuous input of either chemicals or energy for equipment operation (Younger and Banwart, 1999). However, all passive systems require some degree of maintenance during the lifetime of the system. Examples of passive systems include constructed anaerobic or aerobic wetlands (Hedin et al.,1994), reactive walls (Benner et al.,1999) and anoxic limestone drains (Gazea et al.,1996). The main function of reactive walls and anoxic limestone drains is SO_4 reduction and the addition of alkalinity respectively, whereas aerobic wetlands are designed for removal of dissolved Fe(II). Although passive treatment for Fe removal using constructed wetlands requires little ongoing human intervention, the large area of land needed for effective treatment is an important design constraint (Younger and Banwart, 1999). When land is available then mine waters have been successfully treated using these systems (Hedin et al., 1994). In areas where available land is limited by steep terrain or in areas with suitable land unavailable for acquisition from the landowner, such passive treatment methods are not feasible.

Passive removal of dissolved Fe(II) can also consist of a simple treatment method where emerging mine waters are allowed to discharge over a cascade of steps allowing aeration and effective oxidative precipitation of Fe(III) oxide minerals. The water can be diverted into a settling pond (Best and Aikman, 1983) or allowed to discharge into local watercourses if sufficient removal has occurred. At present there are a large number of near-acid to alkaline mine water discharges in the UK (Banks et al., 1997), where continuous and extensive ochre (Fe(III) oxyhydroxide) accretion occurs on the sediments of receiving water courses, with the water column remaining persistently clear of suspended colloidal material.

The accretion of Fe oxides onto such surfaces can be explained by a well documented reaction mechanism; the rapid adsorption of aqueous Fe(II) species to the Fe oxide mineral surface (Zhang et al., 1992) followed by subsequent surface-catalysed oxidation by dissolved O_2 (Wehrli, 1990) and surface precipitation as an Fe(III) oxide mineral phase. The reaction is irreversible under oxic conditions and allows the direct transformation of adsorbed Fe(II) to freshly formed Fe(III) mineral. Reviews of redox processes relevant to mine water pollution show that this abiotic process is rapid at neutral pH, but slows dramatically below pH 5 (Evangelou and Zhang, 1995; Nordstrom and Southam, 1997). At lower pH values the abiotic reaction is negligible compared to the microbially-mediated oxidation of Fe(II)(aq) by acidophilic chemolithotrophic bacteria such as *Thiobacillus ferrooxidans*.

This study proposes that the surface catalysed autooxidation of Fe(II) species (which the authors term "ochre accretion") may be effectively harnessed within a reactor where surface area is maximised to provide effective passive removal of Fe(II)(aq). Such a process, if effective, would be particularly suited to steep terrain provides suitable hydraulic gradients to deliver discharge streams to the reactors.

A previous study was carried out by Best and Aikman (1983) using such a technology; a tank filled with brushwood as a cascade for aeration and Fe oxide accretion. A fraction of the mine water discharge (0.8 l s^{-1}, [Fe(II)] = ~25 mg l^{-1}) at Kames Colliery in Ayrshire, Scotland, UK was fed through a 2 m high filter reactor with a horizontal cross-sectional area of 1×1 m. Water was collected from the base of the filter reactor and passed into an upward flow settlement tank and then eventually discharged to the River Ayr. Once in place, the system was able to operate unattended except for one operation to remove the Fe oxide that had accumulated within the reactor during the 3 month period of the study. No further maintenance was necessary throughout the

experiment. This treatment system is passive in a similar sense to that of aerobic wetlands where occasional, but not continuous, maintenance is required. A flow diagram of the pilot plant treatment system is shown in Fig. 1.

In that study, samples were taken from the discharge above, and from a settling tank below the filter reactor. The samples were analysed for pH, total Fe(II)(aq) and dissolved O_2. To assess variations in design and performance, the discharge was also fed through separate systems consisting of an upward flow flocculation tank and a settling tank. Sample analyses from the discharges clearly showed that the filter reactor where adsorption and surface catalysed auto-oxidation of Fe(II) was occurring, followed by the settlement tank, was the best system for increasing the DO and reducing the Fe(II)(aq) concentration. Over a 3 month period the filter reactor followed by the settlement tank successfully removed 82% of Fe(II)(aq).

The objective of this modelling study is to conceptualise and mathematically describe the Fe(II) adsorption and surface catalysed auto-oxidation processes within a relatively simple model for such reactor processes, in order to better explore the feasibility of developing a passive reactor for treating ferruginous, alkaline mine water discharges.

1.1. Aqueous speciation and oxidation kinetics of ferrous iron

The auto-oxidation kinetics of Fe(II)(aq) species has been previously reviewed and summarised (see Wehrli, 1990 and included references). Oxidation of Fe(II) by molecular O_2 occurs with a simple one-step electron transfer in which the first step in the 4-electron reduction

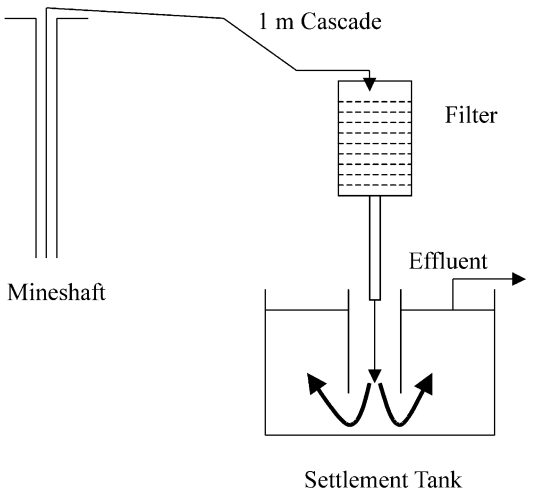

Fig. 1. A diagram of the treatment system at Kames Colliery that was used for model development (described by Best and Aikman, 1983).

of the dioxygen molecule determines the overall rate. Eq. (1) shows the stoichiometry for the overall oxidation of Fe^{2+} ions by O_2.

$$O_2(aq) + 4Fe^{2+} + 6H_2O \leftrightharpoons 4FeOOH(s) + 8H^+ \quad (1)$$

The overall rate of the 4 electron transfer is described by the following general second-order rate law for oxidation of Fe(II), where the subscript i refers to an individual Fe(II) species, and the subscript T refers to the total concentration of Fe(II).

$$\frac{-\mathrm{d}[\mathrm{Fe(II)}]}{\mathrm{d}t}_T = -\Sigma k_i[\mathrm{Fe(II)}]_i[O_2] \quad (2)$$

The second order rate constant for oxidation of Fe(II) adsorbed on mineral surfaces, by O_2(aq), has been estimated by Wehrli (1990) to be of the same order-of-magnitude as that for the $Fe(OH)^+$ hydrolysis species. Subsequent to that study, Zhang et al. (1992) described the aqueous speciation of Fe(II) adsorbed on the surface of Fe oxyhydroxide mineral as surface complexation equilibria. Together, these studies allow the pH dependence of Fe oxidation kinetics, in the presence of sorbing mineral surfaces, to be defined in terms of the pH dependence of aqueous Fe(II) speciation, and the relative rate of oxidation of the various species.

For the pH range considered in the developed model, the following hydolysis species (Wherli, 1990) and surface Fe(II) complexes (Zhang et al., 1992) are defined for the Fe^{2+}–H_2O–FeOOH(s) system. The notation XFeOH refers to a single adsorption site on the uncharged mineral surface of FeOOH(s).

$$Fe^{2+} + H_2O \leftrightharpoons FeOH^+ + H^+ \qquad \log K_1^* = -10.3 \quad (T = 25°C,\ I = 0.1\ \mathrm{M}) \quad (3)$$

$$Fe^{2+} + 2H_2O \leftrightharpoons Fe(OH)_2(aq) + 2H^+ \qquad \log K_2^* = -22.2 \quad (T = 25°C,\ I = 0.1\ \mathrm{M}) \quad (4)$$

$$Fe^{2+} + XFeOH \leftrightharpoons XFeOFe(II)^+ + H^+ \qquad \log^s K_1^* = -1.99 \ (T = 25°C,\ I = 0.1\ \mathrm{M}) \quad (5)$$

$$Fe^{2+} + XFeOH + H_2O \leftrightharpoons XFeOFe(II)OH + 2H^+ \qquad \log^s K_2^* = -8.39 \ (T = 25°C,\ I = 0.1\ \mathrm{M}) \quad (6)$$

Table 1 shows the stoichiometry of the processes and Table 2 lists the second order rate constants for reaction of Fe^{2+} species with dissolved O_2. Inspection of the rate constants demonstrates that the hydrolysis species

Table 1
Reaction stoichiometry for oxidation of dissolved and adsorbed Fe(II) species

Iron(II)(aq) species	Stoichiometric reaction
1. Aquo ion	$4Fe^{2+} + O_2 + 4H^+ \rightarrow 4Fe^{3+} + 2H_2O$
2. Mono-hydroxo solution complex	$4Fe(OH)^+ + O_2 + 4H^+ \rightarrow 4Fe(OH)^{2+} + 2H_2O$
3. Di-hydroxo solution complex	$4Fe(OH)_{2(aq)} + O_2 + 4H^+ \rightarrow 4Fe(OH)_2^+ + 2H_2O$
4. Surface Fe(II) complex	$4XFeOFe^+ + O_2 + 4H^+ \rightarrow 4XFeOFe^{2+} + 2H_2O$
5. Surface Fe(II) hydroxo complex	$4XFeOFeOH + O_2 + 4H^+ \rightarrow 4XFeOFeOH^+ + 2H_2O$

Table 2
Rate constants for oxidation of the dissolved and adsorbed Fe(II) species including. Parameters: k_i = second-order rate constant for the reaction $\frac{d[Fe(II)_i]}{dt} = k_i[Fe(II)_i][O_2(aq)]$[a]

Fe(II) species	2nd-order rate constant	
Fe^{2+}	$k_1 = 7.9 \times 10^{-6}$	l mol^{-1} s^{-1}
$Fe(OH)^+$	$k_2 = 25.1$	l mol^{-1} s^{-1} d
$Fe(OH)_{2(aq)}$	$k_3 = 7.94 \times 10^{+6}$	l mol^{-1} s^{-1} d
$XFeOFe^+$	$k_4 = 5.01$	l mol^{-1} s^{-1} d
XFeOFeOH	$k_5 = 5.01$	l mol^{-1} s^{-1} d

[a] Wehrli (1990) estimated the rate constant for adsorbed Fe(II) species. That rate constant is applied to both surface Fe(II)species proposed by Zhang et al. (1992).

$FeOH^+$, $Fe(OH)_2$(aq) and the Fe(II) species adsorbed on the Fe(III) oxide mineral surface are significantly more reactive than Fe^{2+}.

As described by Wehrli (1990), the main effect of hydrolysis and surface complexation is that oxidation of dissolved Fe(II) increases dramatically at circumneutral and near-basic conditions, where these species dominate. This results from the significantly higher rate of electron-transfer when Fe(II) is covalently bound to electron-donating oxyions of the hydroxide ligand. This effect holds either for complexation by OH^- in solution [Eqs. (3)–(4)] or, analogously, by oxyanions associated with the hydrated mineral surface [Eqs. (5) and (6)]. Surface catalysed oxidation of Fe(II) is generally initiated in the presence of Fe(III) oxide surfaces above pH 5, where significant adsorption of Fe^{2+} occurs due to formation of the surface complex $XFeOFe^{2+}$. The presence of mineral oxide surfaces thus extends the pH range where rapid oxidation of Fe(II)(aq) occurs, well into the near-acid region.

The following stoichiometric reaction represents this irreversible (under oxic conditions) transformation of adsorbed Fe(II) to freshly formed Fe oxyhydroxide. A consequence of surface precipitation is conservation of adsorption sites, represented as XFeOH, which react further [Eqs. (5) and (6)] to adsorb Fe(II) species from solution, and catalyse their oxidation on the FeOOH(s) surface [Eq. (7)].

$$4XFeOFe^{2+} + O_2 + 6H_2O \rightarrow 4FeOOH(s) + 4XFeOH + 4H^+ \quad (7)$$

This conservation of sites is attractive when considering possible application to treatment technology since reactive surface area would not decrease with accretion of reaction product, thus extending the lifetime of the catalytic surface.

2. Methodology

2.1. Model development

A mathematical model for the speciation and oxidative precipitation of Fe(II) using the geochemical code Steadyql (Furrer et al., 1989,1990) has been developed. This model formulates slow or irreversible reaction kinetics with empirical rate laws and rapid reversible reactions as speciation equilibrium, for flow through a single completely-mixed reactor at steady state. The code is described in detail by Furrer et al. (1989, 1990) but will be briefly presented here.

The model contains 47 chemical species that are typical of many discharging mine waters. These species interact through fast reactions considered to be at equilibrium. Solution species are considered to be mobile, while adsorbed species are classified as immobile as they are retained on fixed solid mineral surfaces within the system.

Speciation equilibrium is solved by combining mass action laws for formation of individual species and mass balances for all components, and solving iteratively, using initial estimates of the component concentrations. The list of speciation reactions included in the model are given in Table 3. The thermodynamic constants listed are those critically reviewed and reported by Strömberg and Banwart (1994) as conditional constants ($I = 0.1$ M, $T = 25$ °C). The code neglects corrections to conditional thermodynamic constants arising from further changes in the ionic composition of the reacting solutions and from electrostatic interactions between charged mineral surfaces and adsorbing ions. The activity of H_2CO_3* and Fe^3 are fixed by solubility equilibria with the phases

Table 3
Speciation equilibrium and conditional thermodynamic constants (log$K$) reported in Strömberg and Banwart (1994) for 25 °C and 0.1 M ionic strength

Log K	Aqueous phase
−14.5	$H_2O = OH^- + H^+$
1.43	$H^+ + SO_4^{2-} = HSO_4^-$
0.22	$Na^+ + SO_4^{2-} = NaSO_4^-$
0.31	$K^+ + SO_4^{2-} = KSO_4^-$
−6.3	$CO_3^{2-} + H^+ = HCO_3^-$
−1.5	$CO_3^{2-} + 2H^+ = H_2CO_3$
−12.4	$Mg^{2+} + H_2O = MgOH^+ + H^+$
1.47	$Mg^{2+} + SO_4^{2-} = MgSO_4^0$
−13.7	$Ca^{2+} + H_2O = CaOH^+ + H^+$
1.56	$Ca^{2+} + SO_4^{2-} = CaSO_4^0$
2.40	$Ca^{2+} + H^+ + SO_4^{2-} = CaHSO_4^+$
−10.3	$Fe^{2+} + H_2O\text{-}H^+ = FeOH^+$
−22.2	$Fe^{2+} + 2H_2O = Fe(OH)_2^0 + 2H^+$
4.14	$Fe^{2+} + SO_4^{2-} = FeSO_4^0$
2.40	$Fe^{2+} + H^+ + SO_4^{2-} = FeHSO_4^+$
−3.08	$Fe^{3+} + H_2O = FeOH^{2+} + H^+$
−7.07	$Fe^{3+} + 2H_2O = Fe(OH)_2^+ + 2H^+$
−15.5	$Fe^{3+} + 3H_2O = Fe(OH)_3^0 + 3H^+$
−23.6	$Fe^{3+} + 4H_2O = Fe(OH)_4^- + 4H^+$
2.83	$Fe^{3+} + SO_4^{2-} = FeSO_4^+$
3.64	$Fe^{3+} + H^+ + SO_4^{2-} = FeHSO_4^{2+}$
3.84	$Fe^{3+} + 2SO_4^{2-} = Fe(SO_4)_2^-$
−5.93	$Al^{3+} + H_2O = AlOH^{2+} + H^+$
−12.0	$Al^{3+} + 2H_2O = Al(OH)_2^+ + 2H^+$
−19.5	$Al^{3+} + 3H_2O = Al(OH)_3^0 + 3H^+$
−25.2	$Al^{3+} + 4H_2O = Al(OH)_4^- + 4H^+$
1.90	$Al^{3+} + SO_4^{2-} = AlSO_4^+$
1.62	$Al^{3+} + H^+ + SO_4^{2-} = AlHSO_4^{2+}$
3.47	$Al^{3+} + 2SO_4^{2-} = Al(SO_4)_2^-$
Log K Surface complexes	
6.45	$XFeOH + H^+ = XFeOH_2^+$
−8.27	$XFeOH = XFeO^- + H^+$
−1.99	$XFeOH + Fe^{2+} = XFeOFe^+ + H^+$
−8.39	$XFeOH + Fe^{2+} + H_2O = XFeOFeOH + 2H^+$

($CO_{2\ (g)}$) and $Fe(OH)_{3\ (s)}$ respectively. Mass balances for these species are defined by the transport and reaction processes reflected in Eq. (9) below with species concentrations in the reactor fixed by the respective equilibria (see Furrer et al., 1989, 1990 for details). Redox speciation of Fe is included by defining both Fe^{2+} and Fe^{3+} as master species.

The code formulates empirical rate laws and kinetic rate laws defined in terms of relevant species concentration using the following equation. This kinetic formulation holds for conditions that are far from equilibrium as is the case for oxidation of Fe(II) species under an excess of O_2(aq) at the conditions described for these simulations.

$$R = k \prod [X]_i^n \tag{8}$$

k is the relevant rate constant, $[X]_i$ is the concentration of the reactant species, i and n is the reaction order with respect to species i. Mass balance is defined by transport and reaction in a completely mixed reactor at steady-state [Eq. (9)]. Q is water flow rate (dm^3 s^{-1}) and C is concentration (mol dm^{-3}).

$$Q, \text{in}\ \ C, \text{in} = Q, \text{out}\ \ C, \text{out} \pm \text{Reactions} \tag{9}$$

Oxygen diffusion is included in the model to determine the O_2 flux from the atmosphere in to the reactor. This diffusion is described by linear mass transfer kinetics, where the O_2 flux is proportional to the O_2 deficit i.e. the difference between the concentration of dissolved O_2 at saturation under atmospheric conditions (C,equil) and the concentration of dissolved O_2 in the reactor (C, actual) [Eq. (10)]. α is a linear mass transfer coefficient that is proportional to the diffusion coefficient for O_2(g) and the surface area of the reactor media in contact with air, and is inversely proportional to the film thickness of water on the reactor surface through which the gas must diffuse (see Cussler, 1984).

$$\frac{dc}{dt} = \alpha\left(C_{\text{equil}} - C_{\text{actual}}\right) \tag{10}$$

The authors have formulated zero-order reaction rates for the oxidation of Fe^{2+} by neutrophilic Fe oxidising bacteria using rates reported by Emerson and Revsbech (1994: 0.7–1.35×10^{-9} mol cm^3 h^{-1}) that were determined by loss of Fe(II) across a flow-through reactor maintained at relatively low O_2(aq) concentrations (0.16–1.3 mg l^{-1}). Oxidation rates (mol h^{-1}) are reported as normalised to the volume (cm^3) of active biomass. In order to obtain rates with units of mol l^{-1} s^{-1} as used in the simulations, the reactive surface area to water ratio (m^2 l^{-1}) for a reactor was multiplied by an assumed 0.01 m depth of active biomass as attached growth on the reactor media. The resulting biomass to water ratio (m^3 l^{-1}) was then multiplied by the reported microbial oxidation rates and used directly to calculate Fe(II)(aq) removal rates by this process.

2.2. Estimating reactive surface area and $O_2(g)$ mass transfer coefficients

The field data for the reactor shown in Table 4 and described by Best and Aikman (1983) were used to constrain model parameters. The ratio of surface area to water volume and the O_2(g) mass transfer coefficient [α, Eq. (10)] were systematically varied in simulations until the outflow Fe(II)(aq) and O_2(g) concentrations were similar to those at the field site ($Q = 2.9$ m^3 h^{-1}). These parameter values were then tested by running a further simulation corresponding to a different flow rate used at the field site ($Q = 3.8$ m^3 h^{-1}), and comparing simulation

Table 4
Design and operating parameters reported for the reactor in Fig. 1 (Best and Aikman, 1983) and used for model development and subsequent simulations

Reactor parameters	
Reactor media	Brushwood
Inflow	2.9 m^3h^{-1}
Reactor length	10 dm horizontal
Reactor width	10 dm horizontal
Reactor height	20 dm vertical
Reactor cross-sectional area	100 dm^2
Reactor volume	2000 dm^3
Adsorption capacity	6.0×10^{-8} mol l^{-1}
Surface area : water ratio	6.0×10^{-3} m^2 l^{-1}

results with the field data. The values are shown in Table 5. The corresponding adsorption capacity (total concentration of adsorption sites, mol l^{-1}) was calculated by multiplying the surface area to water ratio (m^2 l^{-1}) by the adsorption density of Fe oxide (1.0×10^{-5} mol m^{-2}; Banwart, 1989).

2.3. Model simulations

The performance of the model and this technology was examined by a series of model simulations.

1. The adsorption capacity was increased for a constant inflow. A range of adsorption capacities were chosen (10^{-12}–10^{-1} mol l^{-1}) to illustrate the dependence of reactor performance on surface area and to assess the sensitivity of the model to different adsorption capacities. Reactor dimensions and discharge rates given by Best and Aikman, (1983, see Table 4) and parameter values estimated from the field data as described above, were used for all of the simulations. As simulated Fe removal approached 100% for very high Fe loadings it was necessary, in some cases, to slightly reduce the discharge rate to the reactor as longer residence times result in declining small Fe concentrations, which creates convergence problems for the numerical algorithm (see Furrer et al., 1989). An Fe(II)(aq) concentration of 100 mg l^{-1} and pH of 6.7 was used in the inflow. Hydrogen carbonate ion concentration was not known, and therefore was calculated from the pH and assuming equilibrium with atmospheric PCO_2(g).

2. Again the adsorption capacity was increased as above but the Fe concentrations were varied with a fixed pH as in the previous simulation. To examine the model's performance and sensitivity to different loadings, increasing Fe(II)(aq) concentrations were used in the inflow from 25 to 75 mg l^{-1} in increments of 25 mg l^{-1}. These increments were chosen as many alkaline mine waters which may benefit from this study have Fe(II)(aq) concentrations within this range (Banks et al., 1997).

3. A range of discharging mine waters with significant differences in their chemistry (i.e. Fe(II)(aq) and pH, Banks et al., 1997) were selected with Fe(II)(aq) concentrations ranging from 10.6 to 67.3 mg l^{-1} and pH values ranging from 3.81 to 6.76. Again adsorption capacity was increased. Simulated treatment of these discharges was carried out to assess the influence of mine waters that are both acidic and alkaline on Fe(II) adsorption and surface-catalysed oxidation. These simulations were first carried out using the full set of water quality data available for each discharge, as input to the model. Additional simulations showed that model results were essentially identical to those obtained when considering only aqueous Fe(II) and Fe(III) species, pH, dissolved inorganic C species and O_2(aq) as the dominant reactive species.

4. Additional simulations were carried out to test if concentration gradients within the reactor led to greatly different results from those obtained with a single completely-mixed reactor. For these simulations, the reactor was divided longitudinally into 6 sections of equal length, with the total size corresponding to the reactor dimensions used for simulations assuming a single completely-mixed reactor.

Table 5
A comparison of simulated and measured Fe removal and dissolved oxygen concentration[a]

Simulations used to constrain parameters		Simulations used to test model	
Fe(II)(aq) removal, per cent			
Simulated	96%	Simulated	83%
Field	97%	Field	62%
Dissolved oxygen, per cent of saturation			
Simulated	81%	Simulated	81%
Field	83%	Field	78%

[a] The ratio of reactive surface area to water and the O_2(g) mass transfer coefficient were constrained by the field data (Best and Aikman, 1983) at 6×10-3 m^2 l^{-1} and 1.80 dm^3 s^{-1}, respectively.

3. Results

Fig. 2 shows removal by oxidation of individual Fe species within the reactor, and the total removal resulting from all oxidation processes. An inflow Fe concentration of 100 mg l^{-1} and pH of 6.7, is used. Iron removal is dominated by oxidation of $FeOH^+$ in solution for adsorption capacities below 10^{-6} M. Removal by oxidation of surface species ($XFeOFe^+$, XFeOFeOH), i.e. surface-catalysed oxidation, increases on the log–log scale linearly with adsorption capacity up to values of $S_t = 10^{-5}$ M. At values greater than $S_t = 10^{-6}$ M, surface-catalysed oxidation dominates the removal of Fe(II)(aq). The

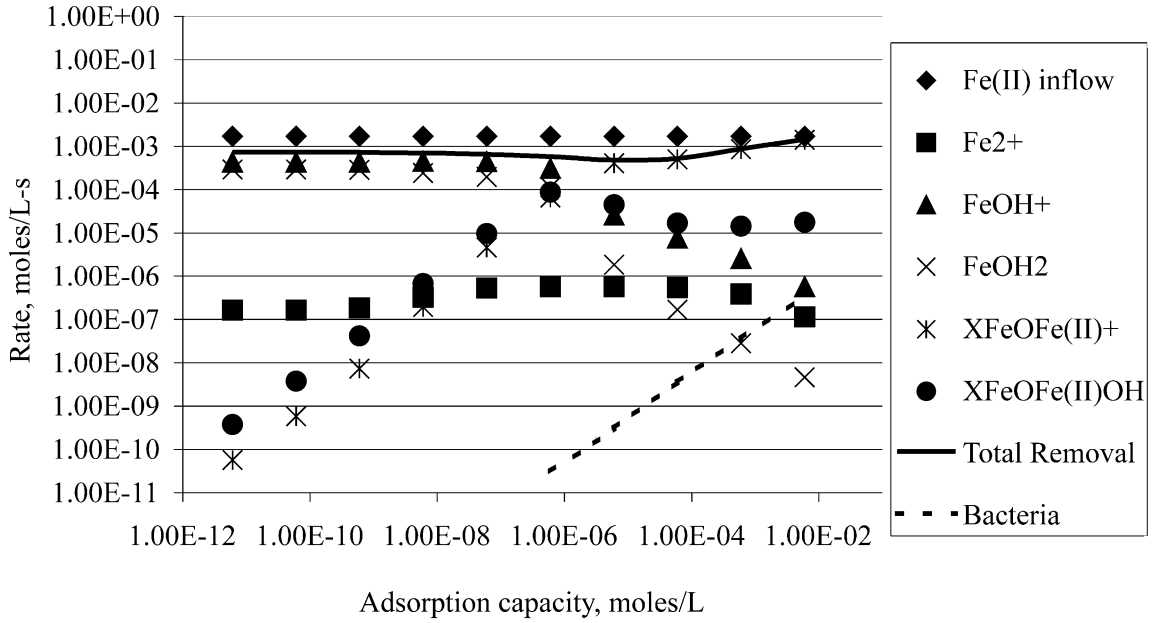

Fig. 2. Rates of oxidation for individual Fe(II) species as a function of adsorption capacity. The plot for Fe(II) Inflow refers to the rate of input of dissolved Fe(II) into the reactor. Discharge characteristics are: 100 mg l^{-1} Fe(II)(aq), pH 6.8, $[HCO_3^-] = 48$ mg l^{-1}, $[O_2(aq)] = 6$ mg l^{-1}.

effect of removing the dissolved Fe load by surface catalysed oxidation is to decrease the concentration of dissolved species and thus their rates of oxidation . The plot shows that the rate of oxidation of $FeOH^+$ drops linearly on the log–log scale with increasing adsorption capacity for values of S_t greater than 10^{-6} M.

In Fig. 2, the removal of Fe(II)(aq) by surface-catalysed oxidation continues to increase with adsorption capacity above values of $S_t = 10^{-5}$ M, although only the removal by oxidation of $XFeOFe^+$ increases. The Fe removal by oxidation of XFeOFeOH actually decreases and then remains constant at values of S_t greater than 10^{-4} M.

At adsorption capacities above 10^{-4} M, the removal of Fe(II)(aq) by surface-catalysed oxidation increases sufficiently to match the load entering the reactor, and essentially complete removal occurs near values of $S_t = 10^{-2}$ M. This demonstrates that if an adsorption capacity greater than 10^{-6} M cannot be engineered in a reactor, then surface-catalysed oxidation will not occur to any significant extent for the Fe loading corresponding to the conditions considered in Fig. 2. Significant removal of dissolved Fe, above that which occurs by oxidation of solution species alone, would require an adsorption capacity near 10^{-2} M to be engineered into a reactor for these conditions.

Fig. 2 also shows the rate of microbial oxidation of Fe^{2+} to be several orders-of-magnitude slower than the abiotic oxidation processes. This result suggests that the microbial processes can be neglected under the reactor conditions that are simulated here. However, these estimates of microbial oxidation rate are uncertain since they assume a zero order reaction extrapolated from conditions of very low $O_2(aq)$ concentration.

Fig. 3 shows the removal efficiency for a range of Fe(II)(aq) loadings including 100 mg l^{-1} as a function of adsorption capacity. Increasing concentrations of Fe(II)(aq) entering the reactor require progressively higher adsorption capacities in order to achieve near-complete removal of the Fe load. Near-complete removal requires approximately 10^{-6} M adsorption sites for an influent concentration of 25 mg l^{-1} Fe(II). A much higher adsorption capacity, near 10^{-2} M, is required to remove the higher Fe(II) concentrations. These values compare with an adsorption capacity near 10^{-5} M which can be engineered with plastic biological filter media (Mass Transfer International, trickling filter media, specific surface area of 100 m^2 m^{-3}) that is typically used by the wastewater industry. Inspection of Fig. 2 thus shows that for this adsorption capacity, only the loading corresponding to 25 mg l^{-1} Fe(II) would be completely removed for the listed conditions.

It is important to note that for near complete removal of 25 mg l^{-1} Fe(II), the dissolved concentration of influent Fe(II) is greater than the adsorption capacity by a factor of 45. Complete removal was still achieved despite an apparently unfavourable ratio of dissolved load to adsorption capacity. These ratios in fact play little role in reactor performance. Rapid, reversible adsorption of Fe(II) cannot explain the removal of dissolved Fe. The

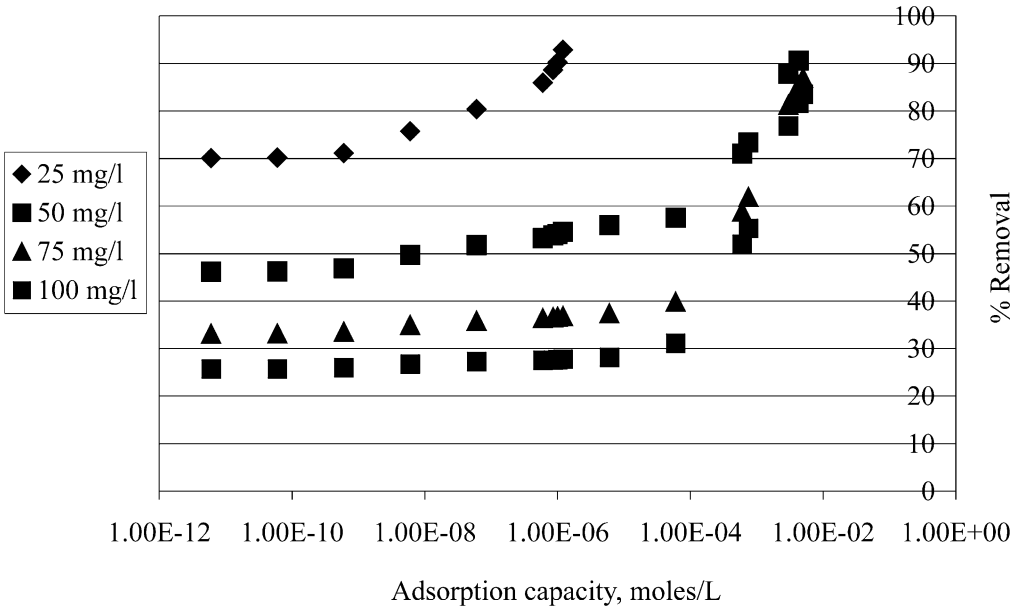

Fig. 3. Calculated Fe removal plotted against adsorption capacity (mol l^{-1}) for reactor influents with 25, 50, 75 and 100 mg l^{-1} Fe(II)(aq), respectively. Discharge characteristics are: 25–100 mg l^{-1} Fe(II)(aq), pH 6.8, $[HCO_3^-] = 48$ mg l^{-1}, $[O_2(aq)] = 6$ mg l^{-1}.

removal is due to the irreversible oxidation of adsorbed Fe(II) to sparingly soluble Fe(III) oxide. The adsorption capacity is only important in the sense of increasing the adsorbed concentration of Fe(II) to levels that allow the surface-catalysed oxidation to proceed sufficiently rapidly to achieve near-complete removal. In the case of removing the 100 mg l^{-1} Fe(II) loading, the adsorption capacity was coincidentally required to be of the same order as the Fe loading. As shown next, influent alkalinity and pH are much more significant than adsorption capacity on reactor performance.

Fig. 4 shows Fe removal as a function of adsorption capacity for the simulated treatment of 4 currently unregulated mine water discharges. Iron removal efficiency decreases with decreasing pH and alkalinity. The extent of removal by surface-catalysed oxidation is complicated by the effect of the resulting acidity generation on pH, and the resulting effect of pH on the adsorption of Fe(II). This is discussed further below, but is demonstrated dramatically by the enormous increase in adsorption capacity required for 100% removal of Fe from the River Hipper (pH 3.81, $[Fe(II)] = 67.3$ mg l^{-1}), compared with that for drainage from Thurcroft Colliery spoil deposits (pH 6.76, $[Fe(II)] = 18.2$ mg l^{-1}).

The impact of acidity and pH on Fe removal is also demonstrated by the results for Dunston Colliery and Allen Spaw discharge. For these, 80% removal is achieved at relatively low adsorption capacity (10^{-6} M), but complete removal requires an adsorption capacity that is an additional 4 orders-of-magnitude greater (10^{-2} M). This increase corresponds directly to increases in acidity due to increased rates of Fe oxidation and precipitation [see Eq. (1)]. The extent of Fe(II) adsorption on Fe oxides depends strongly on pH, decreasing steeply as pH drops into the near-acid pH region. The pH where this decrease in adsorption occurs is termed the adsorption edge and generally falls in the range $5 < pH < 6$ for Fe^{2+} adsorption on Fe(III) oxide. The oxidative precipitation of Fe oxide mineral can drive the reactor pH to values below the adsorption edge for Fe(II), thereby severely limiting Fe(II) adsorption and the rates of surface-catalysed oxidation. Thus, there is a diminishing return on increasing the engineered adsorption capacity in a reactor if there is insufficient alkalinity in the discharge to prevent a drop in pH to values below the adsorption edge.

Fig. 5 shows Fe removal in a column reactor with 6 segments that combine to give a total reactor volume and surface area that is equal to the completely-mixed reactor that was used to generate the greatest Fe removal [90% removal, 100 mg l^{-1} influent Fe(II)] shown in Fig. 3. Iron removal decreases exponentially across the depth of the reactor. Dissolved O_2 concentrations climb within the first reactor segment from an assumed value of 6 mg l^{-1} for a partially aerated discharge feeding the reactor, to 8.46 mg l^{-1}, essentially solubility equilibrium at atmospheric $PO_2(g)$. The drop in pH is significant only in the first few segments where Fe removal is greatest and is therefore, not shown.

A model that assumes that a reactor is completely mixed neglects any concentration gradients within the reactor. In this simplified case, simulated Fe removal

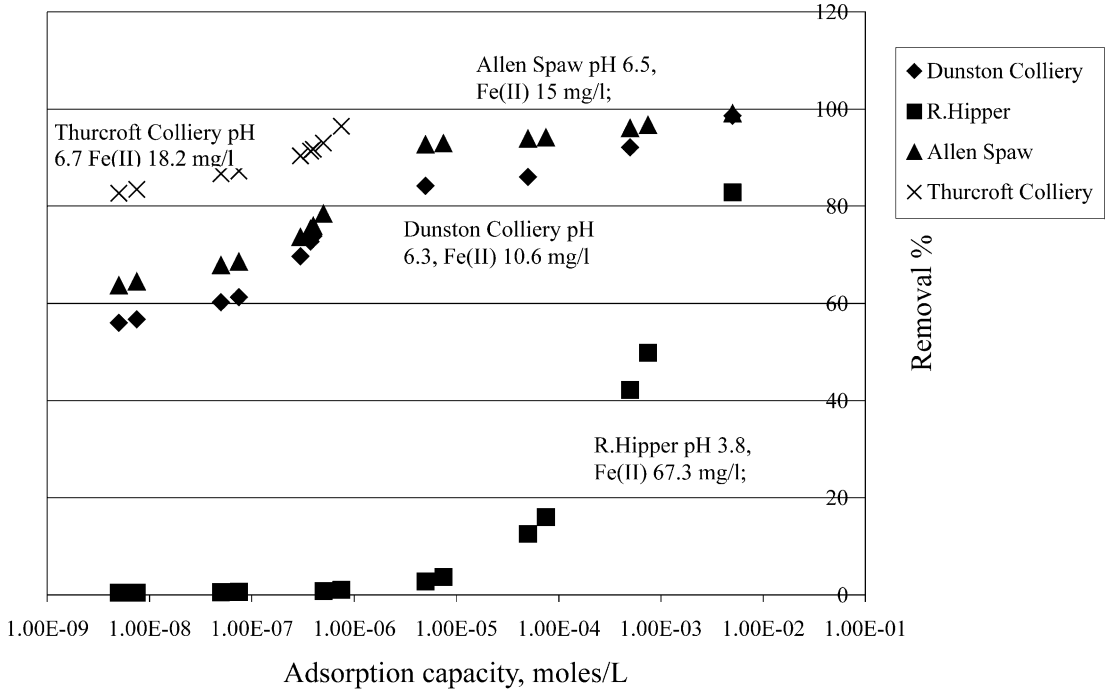

Fig. 4. Removal profiles from selected mine water discharges. Discharge characteristics are 15–67.3 mg l^{-1} Fe(II)(aq), $[HCO_3^-] = 0.0$–60 mg l^{-1}, $[O_2(aq)] = 6$ mg l^{-1}.

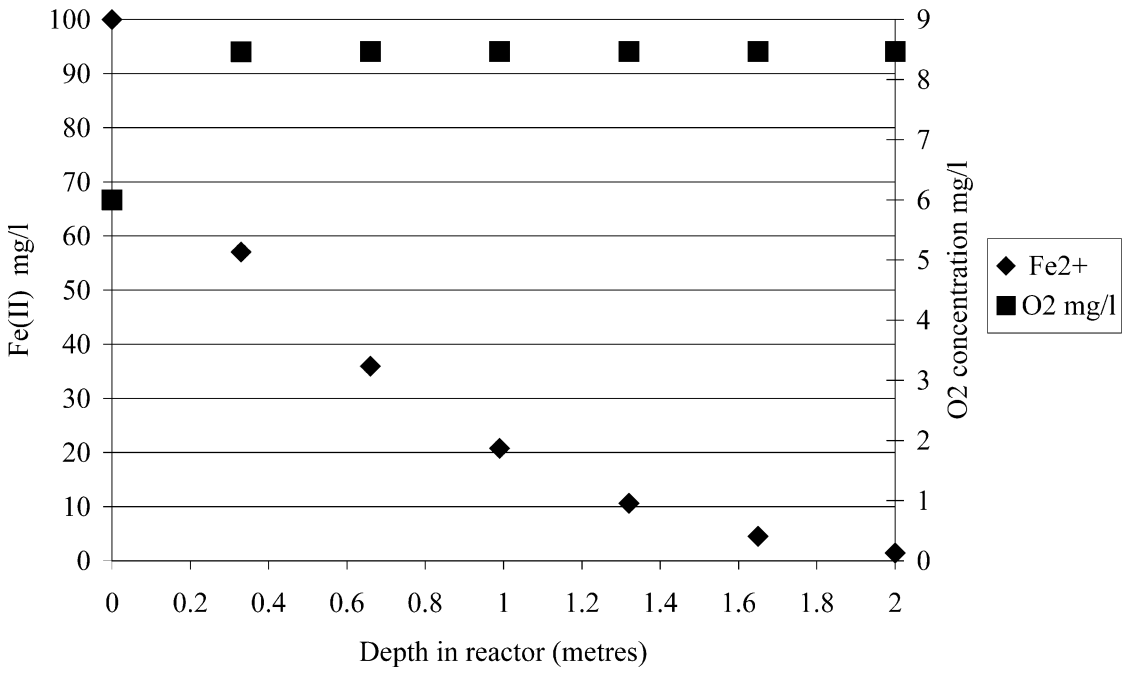

Fig. 5. Fe(II)(aq) concentration as a function of depth in the reactor when modelled as reactors in series in order to simulate a column reactor. Discharge characteristics are: 100 mg l^{-1} Fe(II)(aq), pH 6.8, $[HCO_3^-] = 48$ mg l^{-1}, $[O_2(aq)] = 6$ mg l^{-1}.

rates, which depend on reactant concentrations, are based only on effluent reactant concentrations and are averaged over the entire reactor volume. As shown in Fig. 5, accounting for the concentration gradients expected within a column reactor increases the simulated Fe removal from 90 to 98%. Although trends in performance with engineered adsorption capacity and effluent water quality can be predicted by the completely-mixed reactor, the resulting Fe removal is conservative.

4. Discussion

Fig. 6 shows pH plotted against adsorption capacity for the simulations plotted in Fig. 3 [25–100 mg l^{-1} Fe(II)]. For all of the simulations shown in Figs. 3 and 6 the influent pH and HCO_3^- concentrations were kept constant at values of 6.7 and 48 mg l^{-1}, respectively. Complete removal of dissolved Fe with increasing influent concentrations drives the pH down due to acidity produced by Fe oxide precipitation [Eq. (1)]. This effect is seen clearly in Fig. 6 where increasingly *lower effluent pH* is associated with the near-complete removal of *increasing influent Fe(II)(aq)* concentrations from Fig. 3.

While relatively moderate adsorption capacities are needed to remove 25 mg l^{-1} influent Fe(II) concentration, much higher adsorption capacities are required to remove concentration, 50, 75 and 100 mg l^{-1} (Fig. 3). This is due to the drop in pH discussed above (Fig. 6) which in turn reduces the surface concentration of Fe(II) thus slowing the surface-catalysed oxidation reaction.

Fig. 7 shows the distribution of dissolved and adsorbed Fe(II) species as a function of pH. The plot allows a qualitative comparison of the surface speciation associated with complete removal of influent Fe(II)(aq) under two conditions: (1) an influent concentration of 25 mg l^{-1} with a required adsorption capacity near 10^{-6} mol l^{-1} and (2) influent concentration of 100 mg l^{-1} and adsorption capacity near 10^{-2} mol l^{-1} again associated with essentially 100% removal.

First, inspection of Fig. 6 shows that the reactor effluent corresponding to complete removal of 25 mg l^{-1} Fe(II) is near pH 7.5. Following this, Fig. 7 shows that the mineral surface is dominated by adsorbed Fe(II) at this pH and the rate of surface-catalysed oxidation is relatively rapid. Alternatively, Fig. 6 shows that the reactor effluent corresponding to complete removal of 100 mg l^{-1} Fe(II) is near pH 4.5. This pH value in Fig. 7 shows that the concentration of adsorbed Fe(II) approaches zero relative to dissolved concentrations. The very low surface coverage of adsorbed Fe(II) at low pH therefore requires very high total adsorption capacity for complete removal of Fe(II)(aq). The high adsorption capacity is needed at low pH in order to boost the concentration of Fe(II) surface species into the concentration range where surface catalysed oxidation becomes sufficiently rapid to remove the Fe load.

Of profound influence in adsorption and, therefore, surface-catalysed oxidation, is the influent alkalinity. If sufficient alkalinity is present to maintain circum-neutral or near-basic pH, the reactor performance can be effective. If there is not sufficient alkalinity, then a significant

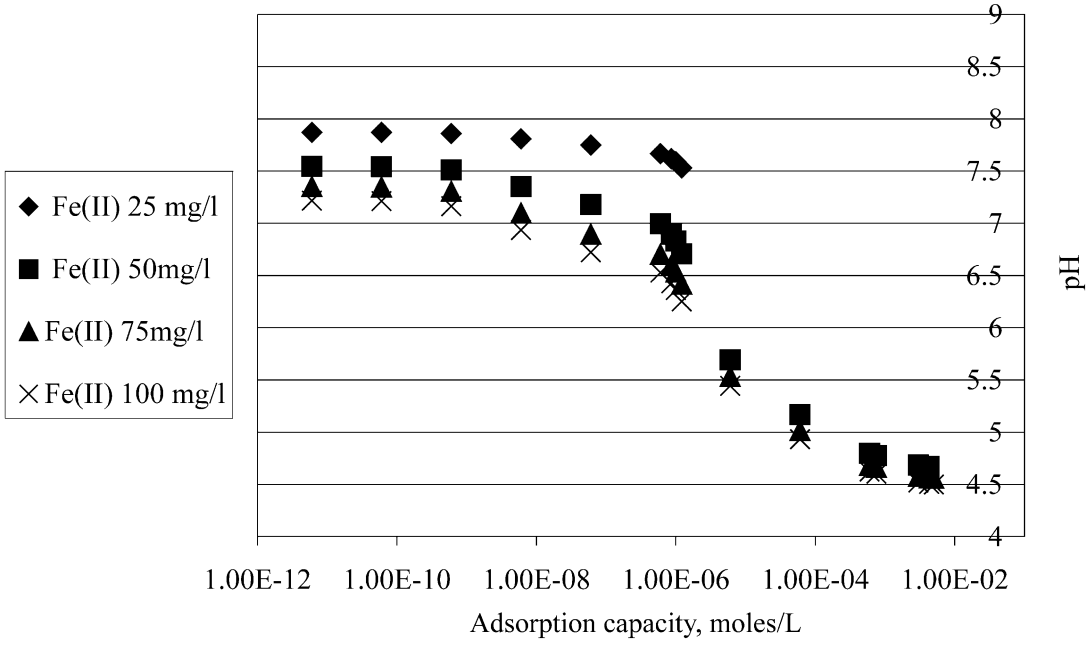

Fig. 6. Effluent pH as a function of Fe(II) concentration and adsorption capacity.

increase in adsorption capacity is required since removal will need to take place at lower pH values where the adsorbed Fe(II) species that drive surface catalysed oxidation are present only in low concentrations.

Alkalinity is defined as the amount of strong acid required to lower the pH to a specified reference value (Schoor and Stumm, 1985). When defining alkalinity according to the carbonate buffer endpoint, the reference value is near pH 5.6 at atmospheric $PCO_2(g)$. When the alkalinity of a solution is positive, the corresponding pH is above this reference value, while negative alkalinity is associated with a pH below the reference value. By coincidence, this reference pH also broadly dictates the efficiency of Fe(II) removal by surface-catalysed oxidation since Fe(II) adsorption occurs strongly at values above pH 6, but is limited below pH 5 (Fig. 7). Therefore, positive values for alkalinity are associated with conditions that favour effective surface-catalysed oxidation, while negative alkalinity (acidity) corresponds to unfavourable conditions for Fe removal.

According to the stoichiometry of reaction (1), each mole of Fe(II) will produce 2 charge equivalents of acidity upon oxidation to Fe(III) hydroxide mineral. Therefore, when calculating alkalinity it is important to realise that hydrolysis and precipitation of metal ions consumes alkalinity due to release of protons, and dissolved Fe^{2+} must be accounted for. Eq. (11) defines alkalinity using this convention.

$$[\mathrm{Alk}] = [\mathrm{HCO_3^-}] + 2[\mathrm{CO_3^{2-}}] + [\mathrm{OH^-}] - 2[\mathrm{Fe^{2+}}] - [\mathrm{H^+}] \quad \text{molar equivalents per litre} \tag{11}$$

Applying Eq. (11) to the influent water quality for the simulations shown in Fig. 3 shows that [Alk] = −2.57 meq l^{-1} and [Alk] = +0.11 meq l^{-1} for influent Fe(II)(aq) concentrations of 100 and 25 mg l^{-1}, respectively. The negative value for alkalinity; i.e. acidity, associated with the higher Fe(II) concentrations, corresponds to a pH range < 5.6, and explains why a much higher adsorption capacity (4 orders of magnitude higher) is required to remove the higher Fe(II)(aq) loading.

For the conditions listed in Fig. 3, approximately 10^{-6} mol l^{-1} adsorption capacity is required to completely remove 25 mg l^{-1} Fe(II). Can a reactor realistically be designed for this removal efficiency? As stated in the results section, plastic trickling filter media would provide on the order of 10^{-5} M adsorption capacity. It would be difficult to dramatically increase the surface area to water volume ratio unless much higher specific surface area filter media could be found. If this is not possible, then removal of higher Fe loadings would require a larger volume of reactor, thus providing a lower hydraulic loading such that sufficient residence time was available to remove the Fe.

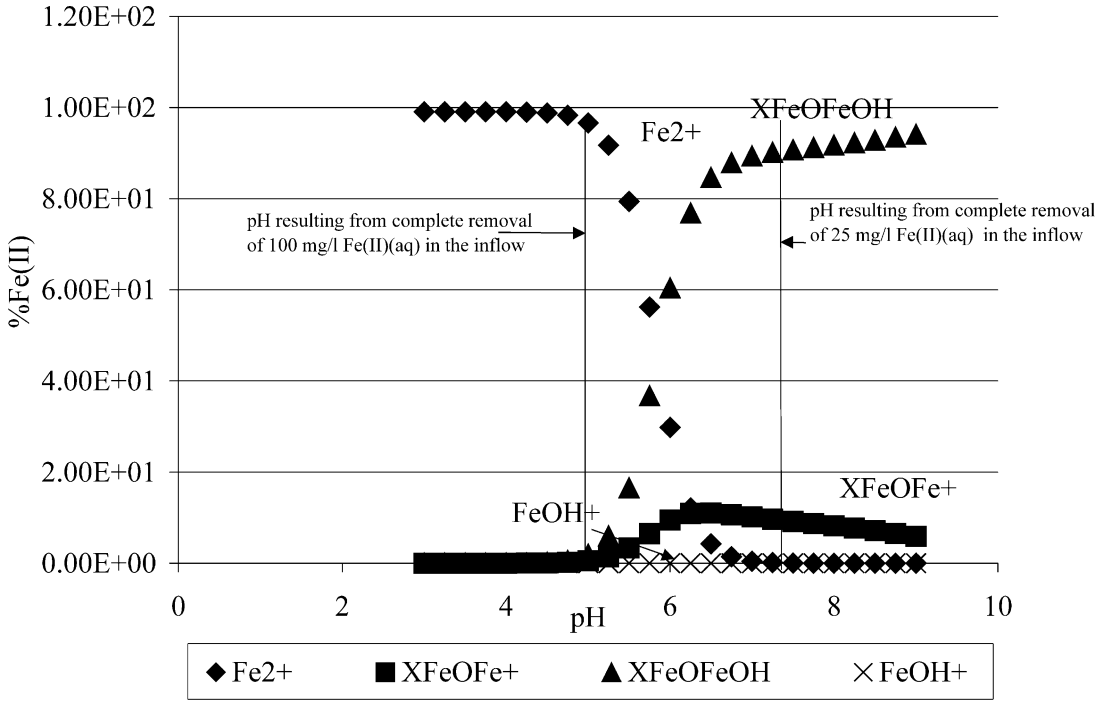

Fig. 7. The distribution of dissolved and adsorbed Fe(II) species as a function of pH.

5. Conclusions

The work reported here shows that a steady state model representing a single completely mixed reactor can be used to represent adsorption and the surface-catalysed oxidation of Fe(II). A simple design concept is to allow a mine water discharge to cascade over filter media allowing aeration and surface catalysed oxidation. The model results suggest that Fe(II)(aq) can be effectively removed if sufficient surface area, and thus adsorption capacity, can be engineered into a reactor.

However, the model has shown that this removal is severely limited by the available alkalinity in the inflow. If there is insufficient alkalinity to buffer the acidity generated by the surface-catalysed oxidation of Fe(II) then a significant increase in adsorption capacity is required. The reactions modelled here are appropriate to assess reactor performance at neutral and basic pH with an excess of O_2(aq), where abiotic Fe oxidation generally dominates over microbially-mediated processes. The alkalinity and pH range of performance may be extended if acidophilic chemolithotrophic bacteria, such as *T. ferrooxidans*, can colonise the reactor surfaces and thrive at low pH conditions.

A completely-mixed reactor is a suitable simplification for assessing the trends in reactor performance with changes in engineered adsorption capacity and influent chemistry, and to gain insight into the engineering science involved. However, detailed modelling for engineering applications may require consideration of concentration gradients within a reactor and their impact on Fe removal. Based on these results for a completely-mixed reactor, pilot studies are planned to assess this technology for the treatment of alkaline ferruginous mine water discharges.

Acknowledgements

The authors wish to acknowledge the Engineering and Physical Sciences Research Council (EPSRC GR/L54790), the UK Coal Authority and International Mining Consultants Ltd. for financial support and Paul Younger and Adam Jarvis (University of Newcastle, UK) for creative input to this work.

References

Appelo, C.A.J., Postma, A., 1996. Geochemistry, Groundwater and Pollution. Balkema.

Banks, D., 1996. The Hydrochemistry of Selected Coal Mine Drainage and Spoil Tip Run-off Waters, Longyearbyen, Svalbard. Norges Geologiske Undersokelse Report 96.141. Trondheim, Norway.

Banks, D., Burke, S.P., Gray, C., 1997. The hydrogeochemistry of coal mine drainage and other ferruginous waters in North Derbyshire and South Yorkshire, UK. Quart. J. Engin. Geol. 30, 257–280.

Banwart, S.A., 1989. The Reductive Dissolution of Hematite (α- Fe_eO_3) by Ascorbate. PhD thesis, Federal Institute of Technology Zurich.

Benner, S.G., Blowes, D.W., Gould, W.D., Herbert, R.B., Ptacek, C.J., 1999. Geochemistry of a permeable reactive barrier for metals and acid mine drainage. Environ. Sci. Technol. 33, 2793–2799.

Best, G.A., Aikman, D.I., 1983. The treatment of ferruginous groundwater from an abandoned colliery. Water Pollution Control 82, 537–566.

Burke, S.P., Younger, P.L., 2000. Groundwater rebound in the South Yorkshire Coalfield: a first approximation using the GRAM model. Quart. J. Engin. Geol. 33, 149–160.

Cheong, Y.W., Min, J.S., Kwon, K.S., 1998. Metal removal efficiencies of substrates for treating acid mine drainage of the Dalsung mine, South Korea. J. Geochem. Explor. 64, 147–152.

Clarke, I.C., 1997. Current legislation to manage the impacts of mining on groundwater in South Africa. In: Hiscock, K., Younger, P., Morris, B., Puri, S., Nash, H., Aldous, P., Tellam, J., Kimblin, R., Chilton, J., Hennings, S. (Eds.), Groundwater in the Urban Environment: Problems, Processes and Management. Balkema, Rotterdam, pp. 567–571.

Cravotta, C.A., Trahan, M.K., 1999. Limestone drains to increase pH and remove dissolved metals from acidic mine drainage. Appl. Geochem. 14, 581–606.

Cussler, E.L., 1984. Diffusion : Mass Transfer in Fluid Systems. Cambridge University Press, Cambridge.

Emerson, D., Revsbech, N.P., 1994. Investigation of an iron-oxidising microbial mat community located near Aarhus, Denmark: Laboratory studies. Appl. Environ. Microbial. 60, 4032–4038.

Evangelou, V.P., Zhang, Y.L., 1995. A review: pyrite oxidation mechanisms and acid mine drainage prevention. Crit. Rev. Environ. Sci. Technol. 25, 141–199.

Feng, X., Hong, Y., Hong, B., Ni, J., 2000. Mobility of some potentially toxic trace elements in the coal of Guizou, China. Environ. Geol. 39, 372–377.

Furrer, G., Sollins, P., Westall, J., 1990. The study of soil chemistry through quasi-steady-state models: acidity of soil solution. Geochim. Cosmochim. Acta 54, 2363–2374.

Furrer, G., Westall, J., Sollins, P., 1989. The study of soil chemistry through quasi-steady-state models: I mathematical definition of problem. Geochim. Cosmochim. Acta 53, 595–601.

Gazea, B., Adam, K., Kontopoulos, A., 1996. A review of passive systems for the treatment of acid mine drainage. Minerals Engin. 9, 23–42.

Hedin, R.S., Narin, R.W., Kleinmann, R.L.P., 1994. Passive Treatment of Coal Mine Drainage. US Bureau Mines Information Circ. IC 9389, US Dept. of the Interior.

Kirby, C.S., Thomas, G., Southam, G., Donald, R., 1999. Relative contributions of abiotic and biological factors in Fe(II) oxidation in mine drainage. Appl. Geochem. 14, 511–530.

Licsko, I., Lois, L., Szebenyi, G., 1999. Tailings as a source of environmental pollution. Water Sci. Technol. 39, 333–336.

National Rivers Authority (NRA), 1994. Water Quality Series No 14, NRA, HMSO, London.

Nordstrom, D.K., Southam, G., 1997. Geomicrobiology of sulfide mineral oxidation. In: Reviews in Mineralogy, Vol. 35. American Mineralogical Society, Washington, DC, pp. 361–390.

Sadler, P.J.K., 1998. Minewater remediation at a French zinc mine: sources of acid mine drainage and contaminant flushing characteristics. In: Mather, J., Banks, D., Dumpleton, S. and Fermor, M. (Eds.), Groundwater Contaminants and their Migration. Geol. Soc. Spec. Publ. 128, 101–120.

Schoor, J.L., Stumm, W., 1985. Acidification of aquatic and terrestrial systems. In: Stumm, W. (Ed.), Chemical Processes and Lakes. John Wiley & Sons, New York.

Stromberg, B., Banwart, S., 1994. Kinetic modelling of geochemical processes at the Aitik mining waste rock site in northern Sweden. Appl. Geochem. 9, 583–595.

Wehrli, B., 1990. Redox reactions of metal Ions at mineral surfaces. In: Stumm, W. (Ed.), Aquatic Chemical Kinetics. Wiley-Interscience, New York, pp. 311–336.

Younger, P.L., 1997. The longevity of minewater pollution a basis for decision making. Sci. Total Environ. 194/195, 457–466.

Younger, P.L., Banwart, S.A., 1999. Mine Waste and Mine Water Pollution Short Course. The Mining Institute, Newcastle upon Tyne.

Zhang, Y., Charlet, L., Schindler, P.W., 1992. Adsorption of protons, Fe(II) and Al(III) on lepidocrocite (γ- FeOOH). Colloid Surfaces 63, 259–268.